Self oscillating PWM modulators, a topological comparison

Poulsen, Søren; Andersen, Michael A. E.

Published in:
Conference Record of the Twenty-Sixth International Power Modulator Symposium, 2004 and 2004 High-Voltage Workshop.

Link to article, DOI:
10.1109/MODSYM.2004.1433597

Publication date:
2004

Document Version
Publisher's PDF, also known as Version of record

SELF OSCILLATING PWM MODULATORS, A TOPOLOGICAL COMPARISION

S. Poulsen[ξ], **M. A. E. Andersen**[ζ]
Ørsted·DTU, Automation, Technical University of Denmark
Elektrovej, Building 325, 2800 Lyngby, Denmark

Abstract

High precision control of the output voltage or current of a switch mode converter with fast response is required for a number of applications. Dependent on the type of application, the desired precision and transient response can be difficult, if not impossible, to achieve with standard Pulse Width Modulation (PWM) control caused by limitations in dynamic capabilities which often limits fast tracking of a reference signal, or fast settling during load steps due to too small achievable control loop bandwidth.
Achievable open loop bandwidth for standard voltage and current mode PWM modulators is typical in the $f_s/10$ or f_s/π range respectively, where f_s is the switching frequency of the converter. For some applications this will require unacceptable high switching frequency to achieve enough control loop bandwidth for the desired dynamic performance.
With self oscillating modulators, the open loop bandwidth is equal to f_s which makes this type of modulators an excellent choice for a wide range of applications. Self oscillating PWM modulators can be made in a number of ways, either as voltage or current mode modulators, and the self oscillating behavior can be achieved either by using hysteresis control or by shaping the open loop function of the modulator so its gain and phase response causes a closed loop natural oscillation. The two main types of self oscillating modulators have many similarities, but differences in dynamic performance and linearity are present.
The work presented is related to the author's work with switch mode audio power amplifiers, where linear tracking of the reference signal is of major importance. Use of the modulator topologies presented are not limited to this kind of equipment, but can be used in a very wide range of applications from very low to very high power levels.

I. 1st ORDER SELF OSCILLATING MODULATORS

Self oscillating modulators use no externally generated carrier signal fed into a comparator, but are basically a closed loop circuit with gain and phase characteristics that ensures a closed loop oscillation. That means 0dB open loop gain at the frequency where the phase shift of the open loop function is -180°.

1st order self oscillating modulators are characterized by an open loop gain function as an integrator, which by itself results in -90° of phase shift. The phase response is modified by introducing a time delay, which is equal to a linear phase shift. The oscillation starts automatically when the additional phase shift caused by the time delay approaches -90°.

B. Hysteresis modulators

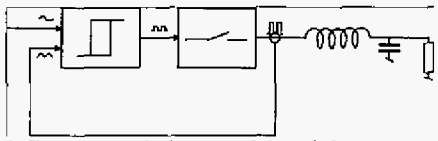

Figure 1 Current mode hysteresis modulator

Figure 1 shows a basic current mode hysteresis modulator [1]. The inductor current is the integral of the difference between the output voltage of the power stage and the output voltage. The measured value of the inductor current is subtracted from the reference voltage, and fed into a hysteresis window to generate the PWM signal. Since the reference voltage controls the low frequency part of the output current, the modulator is a voltage controlled current source.
The hysteresis window adds a controlled time delay equal to:

$$t_d = \frac{V_{hyst}}{\alpha_{carrier}} \qquad (1)$$

where V_{hyst} is the height of the hysteresis window and $\alpha_{carrier}$ is the gradient, or slope, of the carrier.

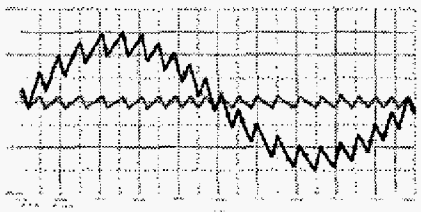

Figure 2. Current mode hysteresis modulator, inductor current and carrier waveform, M=0.5

Figure 2 shows inductor current and carrier waveforms for the current mode hysteresis modulator in Figure 1 with a modulation index, M, of 0.5 . The modulation index is the ratio between output voltage and power supply voltage. At zero output, the carrier waveform is a pure triangle, but at higher M, the carrier waveform change into a sawtooth shaped signal. This is due to the integration made by the inductor of the voltage across it.

[ξ] email: spo@oersted.dtu.dk
[ζ] email: ma@oersted.dtu.dk

0-7803-8586-1/04/$20.00 ©2004 IEEE

As it is seen in Figure 2, the switching frequency drops at high M due to the integration of a smaller voltage across the inductor, resulting in a flatter slope of the carrier signal, giving a greater time delay, before the threshold of the hysteresis window is met, thus reducing the frequency where the -180° of phase shift is met. The switching frequency of the current mode hysteresis modulator is given by:

$$f_s(M) = \frac{V_S}{4} \cdot \frac{1-M^2}{L \cdot I_{Hyst} + \frac{1}{2} \cdot t_d \cdot V_S \cdot (1+M^2)} \quad (2)$$

where V_S is the power supply voltage, I_{hyst} is the height of the hysteresis window, L the inductor value and t_d the time delay trough the modulator loop.

It is seen that if the height of the hysteresis window is made from the power supply rails, the switching frequency will be independent of the value of the supply rails. At higher M, the carrier shape deviates from straight slopes as illustrated in Figure 3.

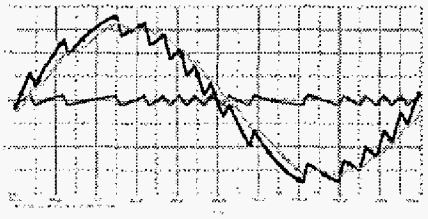

Figure 3. Current mode hysteresis modulator, output voltage, inductor current and carrier waveform, M=0.8

Since the slope of the carrier is the integral of the voltage across the inductor, the slope is sensitive to the ripple voltage on the output of the modulator. When the switching frequency drops, the output ripple voltage gets comparable to the inductor voltage, and the slope of the carrier becomes smaller, degrading the performance of the modulator. In most applications the maximum modulation index of the modulator should be limited to appr. 0.8, keeping a minimum switching frequency and thereby keeping a good performance.

C. Voltage mode hysteresis modulators

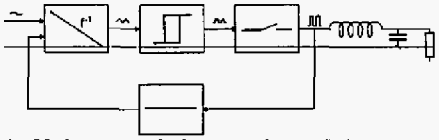

Figure 4. Voltage mode hysteresis modulator

Figure 4 shows the basic voltage mode hysteresis modulator [2], or AIM, Astable Integrating Modulator. The basic operation is the same as for the current mode hysteresis modulator except that the integrating element is an active integrator, integrating the voltage difference between the output voltage of the power stage and the reference voltage, thus making the modulator a filterless voltage controlled voltage source. The switching frequency is determined by:

$$f_s(M) = \frac{V_S}{4} \cdot \frac{1-M^2}{\tau_{int} \cdot V_{hyst} + \frac{1}{2} \cdot t_d \cdot V_S \cdot (1+M^2)} \quad (3)$$

where τ_{int} is the time constant for the integrator, and V_{hyst} is the height of the hysteresis window.

The voltage mode hysteresis modulator has the same dependence of the modulation index as for the current mode hysteresis modulator.

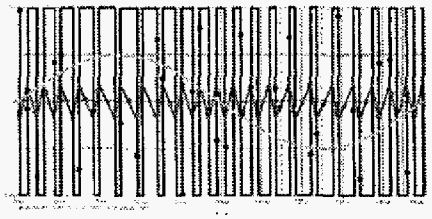

Figure 5. Voltage mode hysteresis modulator, power stage output voltage, carrier waveform and reference, M=0.5

D. 1st order fixed delay self oscillating modulators

A 1st order fixed delay modulator can easily be implemented by removing the hysteresis block in a hysteresis modulator. The additional -90° of phase shift to start the oscillation will be determined by the time delay of the modulator loop only, thus giving the switching frequency:

$$f_s(M) = \frac{1}{2} \cdot \frac{1-M^2}{t_d \cdot (1+M^2)} \quad (4)$$

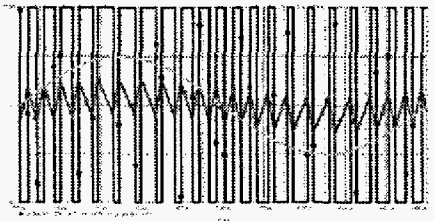

Figure 6. Self oscillating modulator with propagation delay control of switching frequency, power stage output voltage, carrier waveform and reference, M=0.5

As it is seen in Figure 6, the carrier signal correspond to the carrier signal of the hysteresis modulators, except that it is summed with the reference voltage, but the switching frequency's dependence on M is the same as for the hysteresis modulators.

E. nth order self oscillating modulators

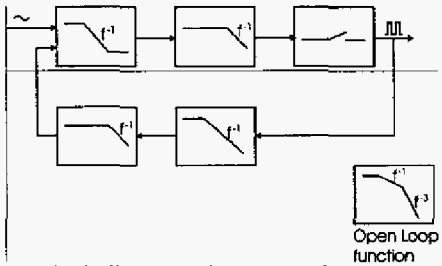

Figure 7. Block diagram of COM modulator

Figure 7 shows the COM, Controlled Oscillation Modulator [3]. The open loop function is shaped with a dominant low frequency pole, resulting in -90° phase shift at high frequencies. Two additional high frequency poles

are inserted at the frequency where the open loop gain equals 0dB, each contributing with additional -45° of phase shift, making the total phase shift -180°, thus causing a natural oscillation when the loop is closed. The overall properties for the COM modulator is fairly similar to the voltage mode hysteresis modulator, except that the carrier at idle is close to sinusoidal because of the larger attenuation of the frequencies above the switching frequency, decreasing linearity and dynamic capabilities by changing the open loop function from a 1st order to a 3rd order function at high frequencies.

II. COMPARISION OF SELF OSCILLATING MODULATORS

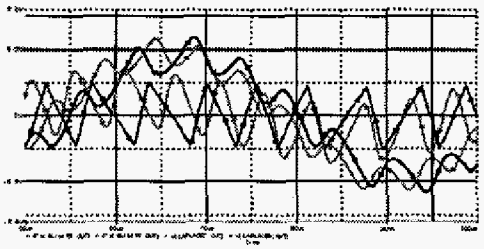

Figure 8. COM (light), AIM (dark) carrier and output waveforms, fin=20kHz, M=0.5, fs, idle=200kHz

Figure 8 shows simulated carrier and output waveforms (60kHz L-C output filter applied) for COM and AIM modulators at M=0.5. The modulators are equally designed, using same characteristic frequencies and 200ns total loop propagation delay. The difference in shape of the carrier waveforms is clear.

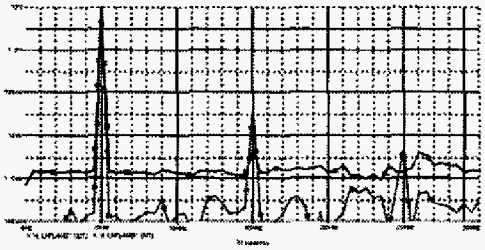

Figure 9. FFT, COM (light), AIM (dark), fin=5kHz, M=0.8, fs, idle=200kHz

Figure 9 shows a simulated FFT of the output of the modulators in Figure 8 at M=0.8. The difference in linearity shows clearly the importance of a carrier waveform with linear slopes.

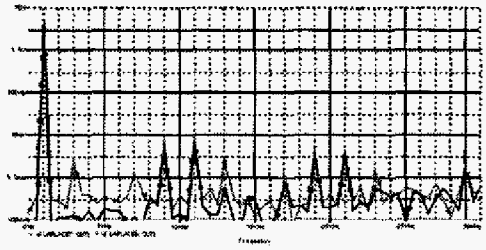

Figure 10. PSRR, COM (light) and AIM (dark), fin=1kHz, M=0.4, PS=+/-40% @ 10kHz, fs, idle=200kHz

Figure 10 shows simulated power supply ratio, PSRR, for the two modulators in Figure 8, with a +/-40% variation @10kHz of the power supply rail. It is seen that the fundamental of the supply variation is not present in the output spectrum, why self oscillating modulators some time is referred to as having infinite PSRR [4], but intermodulation products occur between the reference signal and the supply variation. These intermodulation products are of lowest number and value with the AIM modulator.

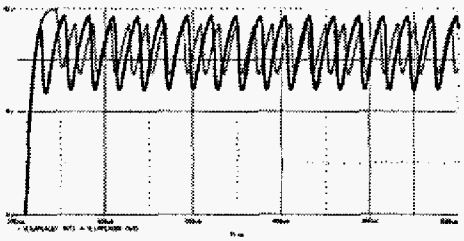

Figure 11. Step response, COM (light), AIM (dark), saturated-M=0.8, fs, idle=200kHz

Figure 11 shows simulated step response of the modulators in Figure 8. The simulation starts with overloaded, saturated modulators, changing to operation at M=0.8. The true first order behavior without any overshoot should be noticed with the AIM modulator which also have the fastest response time.

III. CARRIER DISTORTION

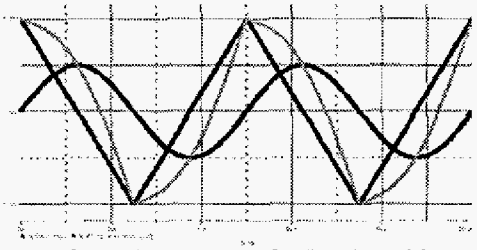

Figure 12. Control output, "Perfect" and resulting carrier

Figure 12 shows some waveforms illustrating the definition of carrier distortion for a standard PWM example. Dark gray is an undistorted triangular carrier and the output voltage of the additional control feedback loop, and light gray is the resulting, effective carrier. The high frequency content of the control loop output is in this example simplified to only the switching frequency, and none of its harmonics. A phase shift of 90° is added to the control output with respect to the triangular carrier. It is seen that the carrier is heavily distorted, resulting in a non-linear modulation caused by the non constant gain of the modulation.

$$K_M = \frac{1}{V_P} \cdot \frac{d_{vc}(t)}{dt} \cdot \frac{2}{T} \qquad (5)$$

The modulator gain K_M is a function of the carrier amplitude V_P and carrier voltage $V_C(t)$. It is seen that K_M is strongly dependent on the shape of the carrier. Any deviation on the carrier shape from the perfect triangle

with constant slopes changes K_M, that is if the carrier have acceleration on the slopes.

Figure 13 illustrates the non linear modulator gain caused by carrier distortion. The figure shows the two carrier waveforms from Figure 12 and the corresponding modulator for one half switching period. Due to symmetry, the modulator gain will be repeated for the other half of the switching period. The two carrier signals are the solid traces, and the corresponding gains the dotted traces. Dark traces correspond to the clean carrier and light to the effective. It is clearly seen that the gain of the modulation itself becomes a highly nonlinear when the effective carrier signal is no longer a clean triangle.

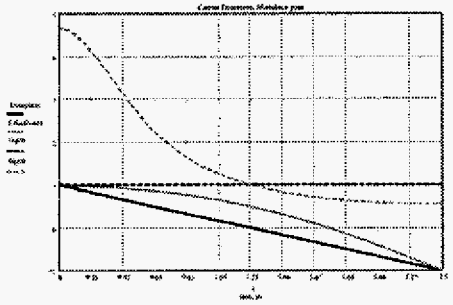

Figure 13. Carrier distortion, modulator gain

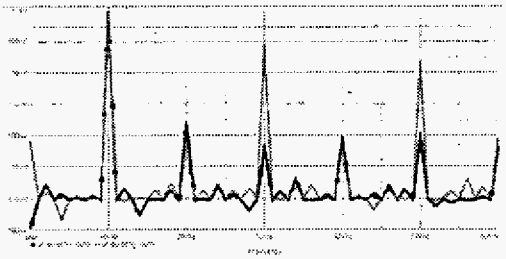

Figure 14. FFT spectrum for modulation with "perfect" and resulting carrier, M=0.8

Figure 14 shows the FFT spectrum for a 10kHz reference signal modulated with the ideal and the effective carrier in Figure 12. The differences in the level of the harmonics are clearly shown, indicating that special care should be taken to the carrier cleanliness when adding additional control feedback loops.

F. Shaping control loop and modulator

For some application one or mere additional control feedback loop(s) are required for suppressing distortion components, giving higher linearity. However, the output of such feedback will have a high frequency content, which effectively will add to the carrier, thus changing its waveform. By designing the inner modulator loop in such a way that it only partly full fill the requirements for a true 1st order behavior, the control loop can be designed in such a way that the high frequency content of its output exactly corresponds to the portion the modulator loop deviates from the true integrating behavior.

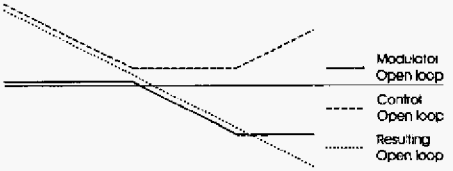

Figure 15. Combining inner and outer loop functions

Figure 15 illustrates how the inner modulator loop and the outer control loop can be shaped to achieve the desired, pure 1. order function for the combined circuit. This will be met if the phase of the control loop is shifted 180° with respect to the phase of the controller loop at high frequencies, ensuring generation of a perfect sawtooth shaped carrier signal.

In Figure 16 is shown the definition of the open loop functions in Figure 15. MFW and MFB is the controller forward and feedback blocks, CFW1-N and CFB is the control forward and feedback blocks. Dotted lines indicate optional system blocks.

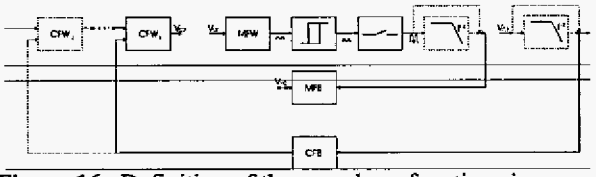

Figure 16. Definition of the open loop functions in Figure 15

IV. EXPERIMENTAL RESULTS

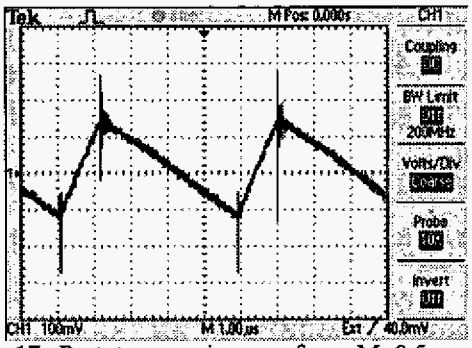

Figure 17. Prototype carrier waveform, M=0.5

Figure 17 shows the carrier waveform for a prototype implementation of a hysteresis modulator with an additional control feedback loop shaped as illustrated in Figure 15 and 16, with M=0.5. The resulting carrier waveform is perfect with straight slopes.

V. CONCLUSION

For self oscillating modulators, linear carrier waveform is shown to be important in terms of linearity and transient behavior. Furthermore a concept for adding additional control loop gain to improve overall system linearity is described. The concept allows adding control feedback loop(s) without changing the resulting carrier waveform and thereby take full benefit of the additional loop gain, thus maintaining the desired linear operation.

VI. ACKNOWLEDGEMENTS

The work presented in this paper is some of the results from an on-going Ph.D. research project, ACT - ACtive Transducers, at Technical University of Denmark, financed by The Danish Energy Authority, journal number 1273/01-006. The project is in co-operation with Bang & Olufsen ICEpower A/S and Danish Sound Technology A/S.

VII. REFERENCES

[1] Robert W. Erickson, Dragan Maksimovic: Fundamentals of Power Electronics, Second Edition, 2001, ISBN 0-7923-7270-0, page 657-659

[2] ELBO GmbH: Selbstshwingender Digitalverstärker, DE 198 38 765 A1, German patent May, 2000

[3] Karsten Nielsen: Pulse Modulation Amplifier with Enhanced Cascade Control Method, WO98/19391, Int. patent, May 1998

[4] Karsten Nielsen, Lars Michael Fenger: The Active pulse modulated Transducer (AT) A novel audio power conversion system architecture, AES 115th convention paper, 2003